PHYSICAL REVIEW B, VOLUME 65, 035202

Dielectric response of molecules in empirical tight-binding theory

Timothy B. Boykin
Department of Electrical and Computer Engineering, University of Alabama in Huntsville, Huntsville, Alabama 35899

P. Vogl
Walter Schottky Institute, Technische Universität München, D-85748 Garching, Germany

(Received 10 July 2001; published 13 December 2001)

In this paper we generalize our previous approach to electromagnetic interactions within empirical tight-binding theory to encompass molecular solids and isolated molecules. In order to guarantee physically meaningful results, we rederive the expressions for relevant observables using commutation relations appropriate to the finite tight-binding Hilbert space. In carrying out this generalization, we examine in detail the consequences of various prescriptions for the position and momentum operators in tight binding. We show that attempting to fit parameters of the momentum matrix directly generally results in a momentum operator which is incompatible with the underlying tight-binding model, while adding extra position parameters results in numerous difficulties, including the loss of gauge invariance. We have applied our scheme, which we term the Peierls-coupling tight-binding method, to the optical dielectric function of the molecular solid PPP, showing that this approach successfully predicts its known optical properties even in the limit of isolated molecules.

DOI: 10.1103/PhysRevB.65.035202 PACS number(s): 71.15.Ap, 71.20.Rv, 31.10.+z

I. INTRODUCTION

The empirical tight-binding method owes much of its long success to the fact that it provides a physically transparent, computationally efficient approach to electronic structure calculations for crystalline systems.[1–3] The method has been extended to include electromagnetic fields, permitting the calculation of observables such as the dielectric function for crystalline solids.[4–6] The empirical tight-binding method is not inherently restricted to crystalline solids and, in view of the growing importance of molecular electronics and biophysics applications, extending the method to encompass electromagnetic interactions in molecules is timely.

Because molecular systems can exhibit characteristics of both periodic solids and isolated molecules, tight-binding calculations of their optical properties vividly illustrate the subtleties of the momentum operator, through which the vector potential couples into the Hamiltonian. These subtleties arise from the finite dimension of the tight-binding Hilbert space, which cannot accurately represent $\hat{\mathbf{p}} \rightarrow -i\hbar\nabla$, and whose operators (represented by finite matrices) cannot satisfy the complete-basis commutation relations $[\hat{r}^{(\alpha)},\hat{p}^{(\beta)}] = i\hbar\hat{1}\delta_{\alpha,\beta}$ since in a finite basis $\mathrm{Tr}(\hat{r}^{(\alpha)}\hat{p}^{(\beta)}) = \mathrm{Tr}(\hat{p}^{(\beta)}\hat{r}^{(\alpha)})$. Consequently, the relationship between real-space (complete basis) quantum mechanics and empirical tight binding is rather analogous to that between a differential equation and its corresponding finite-difference approximation, and it is clear that the customary textbook equations for most important observables (effective mass, dielectric function, etc.) must be rederived using the appropriate finite-basis commutation relations. Understanding the momentum operator in tight binding is therefore an essential preliminary to treating electromagnetic interactions in molecular systems; it is accordingly the focus of the present paper.

In our previous papers we have taken into account the incompleteness of the tight-binding basis in calculating the effective masses and dielectric functions of crystalline materials.[4–7] The dielectric function is in fact but one application of a general scheme for incorporating electromagnetic fields into the empirical tight binding theory without the introduction of additional parameters.[4–6] Our method, which we call Peierls-coupling tight binding, guarantees gauge invariance and charge conservation, and leads to physically transparent expressions for quantities such as optical response functions and dynamical effective charges.[8,9] Most importantly, it is fully compatible with the underlying (i.e., zero external field) tight-binding model in the sense that the representations of the position and momentum operators we employ in calculating extrinsic properties (e.g, dielectric response) give the correct intrinsic properties such as the velocity (band slope) and inverse effective mass (band curvature).

Others have taken a different approach for treating electromagnetic interactions, arguing for the introduction of extra parameters (*a posteriori*) into tight-binding models to improve agreement with experiment by explicitly providing for intra-atomic transitions; we shall refer to such schemes as enlarged tight-binding methods. Most recently, Pedersen *et al.*[10] have even claimed that our Peierls-coupling tight-binding method is incorrect, does not apply to nonperiodic systems such as molecules, and should be augmented to accommodate intra-atomic transitions by adding an explicit, *k*-independent term to the momentum matrix.[10] Although they are able to achieve good agreement with the Kronig-Penney model, their approach has fatal flaws. As we shall see below, the resulting momentum operator does not give the correct band slopes and leads to artifacts such as non-Hermitian operators, and violation of gauge invariance.

We therefore focus on the role played by the momentum operator in coupling electromagnetic fields into the empirical tight-binding Hamiltonian for both crystalline and molecular systems, with particular emphasis on the consequences of introducing extra parameters. In Sec. II we briefly review our Peierls-coupling tight-binding method and discuss the impli-

0163-1829/2001/65(3)/035202(10)/$20.00

cations of adding parameters to a tight-binding model, i.e., the enlarged tight-binding method. In Sec. III we show that our earlier results derived for crystalline systems[4,6] can be applied in a straightforward manner to molecular systems. As an example we calculate the dielectric susceptibility of the one-dimensional phase of poly(para-phenylene) (PPP) which exhibits characteristics of both periodic and isolated systems. Section IV presents our conclusions.

II. ELECTROMAGNETIC FIELDS IN TIGHT BINDING

Of central importance to any generalization of the empirical tight-binding method to encompass electromagnetic interactions in molecular systems is the treatment of the position and momentum operators. As mentioned in Sec. I, there is some controversy surrounding their correct representations, with the isolated-atom limit often used as the reason for adding extra parameters. In contrast, there has been no discussion of how the incompleteness of the tight-binding basis affects calculations of observables in any method to which extra parameters have been added. Thus, prior to deriving the dielectric function of a molecular system, we briefly review the incorporation of electromagnetic fields in tight binding in the Peierls-coupling tight-binding method and examine the consequences of adding extra position or momentum parameters in enlarged tight-binding models.

A. Peierls-coupling tight-binding method

We summarize here our method[4,6] which does not introduce additional parameters. For the sake of clarity, we discriminate Hilbert space operators such as $\hat{H}$ from matrix representations that we write in the form $\overleftrightarrow{\mathbf{H}}$. Système International (SI) units shall be used throughout. Consider a tight-binding Hamiltonian that is characterized by the on-site and off-site Hamiltonian matrix elements

$$\varepsilon^0_{\alpha I} = \langle \alpha, I | \hat{H}^0 | \alpha, I \rangle,$$

$$t^0_{\alpha' I', \alpha I} = \langle \alpha', I' | \hat{H}^0 | \alpha, I \rangle. \tag{1}$$

Here, the orthonormal basis states $|\alpha, I\rangle$ are labeled by a site index I and a symmetry-related index α that numbers the orbitals at a given site. An electromagnetic field specified by the scalar potential $\Phi(\mathbf{r},t)$ and the vector potential $\mathbf{A}(\mathbf{r},t)$ modifies these matrix elements as follows:

$$\varepsilon_{\alpha I} = \varepsilon^0_{\alpha I} - \Phi(\mathbf{R}_I, t),$$

$$t_{\alpha' I', \alpha I} = t^0_{\alpha' I', \alpha I} \exp\left\{ -\frac{ie}{\hbar} \int_{\mathbf{R}_I}^{\mathbf{R}_{I'}} \mathbf{A}(\mathbf{r},t) \cdot d\mathbf{l} \right\}, \tag{2}$$

where the modification in Eq. (2) is called the Peierls substitution.[4] For a general vector potential there is the question of which path to use in the integral, the straight line being generally adopted for nearest-neighbor models.[4,6] For a well-behaved vector potential using the straight-line path yields matrix elements Eq. (2) identical to those of an explicit (Hermitian) Hamiltonian operator into which $\mathbf{A}(\mathbf{r},t)$ couples.[6] Note that when we employ Eq. (2) in Sec. III below we shall work in the electric dipole approximation, $\mathbf{A}(\mathbf{r},t) = \mathbf{A}(t)$, so that the path issue does not arise.

To date the Peierls substitution has been used very successfully to study nonperturbative interactions of light and matter[11–13] and magnetic band structures.[14–17] So far, it seems not to have been employed in first-principles tight-binding methods[18–21] even though nothing in the Peierls substitution is inherently restricted to empirical models and it should, in principle, be possible to employ it here as well. This would be particularly advantageous for real-space *ab initio* methods that invoke Wannier functions to study nonperturbative effects of electromagnetic fields.[22]

B. Enlarging a model with momentum matrix parameters: A counterexample

In Ref. 10 it is suggested that extra parameters be added directly to the momentum matrix in order to augment the interband momentum matrix elements obtained by the Peierls-coupling tight-binding method. Consider a one-dimensional tight-binding model that has one s and one p orbital per site, with sites separated by a distance a. In the localized orbital basis the Hamiltonian matrix elements are $(\alpha \in \{s,p\})$

$$\langle \alpha; n'a | \hat{H} | \alpha; na \rangle = E_\alpha \delta_{n',n} + U_{\alpha\alpha}(\delta_{n',n+1} + \delta_{n',n-1}), \tag{3}$$

$$\langle p; n'a | \hat{H} | s;\, na \rangle = U_{sp}(\delta_{n',n+1} - \delta_{n',n-1}). \tag{4}$$

In the Bloch basis,

$$|\alpha; k\rangle = \frac{1}{\sqrt{N}} \sum_{n=1}^{N} e^{ikna} |\alpha; na\rangle, \tag{5}$$

where again $\alpha \in \{s,p\}$ and the Hamiltonian matrix is

$$\overleftrightarrow{\mathbf{H}} = \begin{bmatrix} h_{ss}(k) & i h_{sp}(k) \\ -i h_{sp}(k) & h_{pp}(k) \end{bmatrix}, \tag{6}$$

$$h_{ss}(k) = E_s + 2U_{ss}\cos(ka),$$

$$h_{pp}(k) = E_p + 2U_{pp}\cos(ka),$$

$$h_{sp}(k) = 2U_{sp}\sin(ka), \tag{7}$$

with eigenvalues

$$E_{\pm}(k) = \frac{1}{2}\Big[h_{ss}(k) + h_{pp}(k) \pm \sqrt{[h_{ss}(k) - h_{pp}(k)]^2 + 4h_{sp}^2(k)}\Big], \tag{8}$$

and eigenvector corresponding to $E_-(k)$,

$$\mathbf{v}_- = \frac{1}{\sqrt{[h_{ss}(k) - E_-(k)]^2 + h_{sp}^2(k)}} \begin{bmatrix} -i h_{sp}(k) \\ h_{ss}(k) - E_-(k) \end{bmatrix}. \tag{9}$$

In the Peierls-coupling tight-binding scheme, we have the minimal momentum matrix $\overleftrightarrow{\mathbf{p}}_k = (m_0/\hbar)(d\overleftrightarrow{\mathbf{H}}/dk)$, whose expectation value is proportional to the band slope,

$$\mathbf{v}_-^\dagger \overleftrightarrow{\mathbf{p}}_k \mathbf{v}_- = \frac{m_0}{\hbar}\frac{dE_-}{dk}, \tag{10}$$

exactly as it must be for a model without the spin-orbit interaction.[7] (The calculation is tedious but straightforward.) Pedersen *et al.*[10] now introduce an additional momentum matrix to accommodate intra-atomic transitions,

$$\overleftrightarrow{\mathbf{P}} = \begin{bmatrix} 0 & -iP_{sp} \\ iP_{sp} & 0 \end{bmatrix}. \tag{11}$$

While they are indeed able to fit the tight-binding interband matrix element to that of the Kronig-Penney model with Eq. (11) they have thereby rendered the total momentum operator $\overleftrightarrow{\mathbf{p}}_k + \overleftrightarrow{\mathbf{P}}$ useless for any calculations that depend on the electron velocity, such as tunneling or transport. This gross defect of the total momentum operator is obvious, since

$$\mathbf{v}_-^\dagger (\overleftrightarrow{\mathbf{p}}_k + \overleftrightarrow{\mathbf{P}})\mathbf{v}_- = \frac{m_0}{\hbar}\frac{dE_-}{dk} + 2P_{sp}\frac{h_{sp}(k)[h_{ss}(k) - E_-(k)]}{[h_{ss}(k) - E_-(k)]^2 + h_{sp}^2(k)}, \tag{12}$$

where the second term does *not* vanish for all *k*. The total momentum operator now fails to yield the correct carrier velocity and hence has lost its physical meaning.

C. Enlarging a model with position parameters: Errors due to incompleteness

Another suggestion that has been made by several authors[10,23] is to enlarge the interband momentum matrix elements of the Peierls-coupling tight-binding scheme with the same-atom *s*-*p* matrix element of position. While this method, that we will also call an enlarged tight-binding method, does seem attractive on first inspection, it suffers from errors due to the incomplete tight-binding basis arising from products of position operators. This problem cannot be dismissed by considering only the linear response, for, as shown in Sec. III below, even the linear response involves double commutators such as $[\hat{r}^{(x)},[\hat{r}^{(y)},\hat{H}^0]]$. First, however, we briefly describe the method and its initial attraction.

In the model of Sec. II B above one would write the position operator as a sum of two operators $\hat{r}_c + \hat{r}_{\rm inter}$, where $\hat{r}_c$ is the same-atom, same-orbital position operator from tight binding without additional parameters and $\hat{r}_{\rm inter}$ is the new (purely interband) same-atom *s*-*p* interaction. The unique nonvanishing matrix elements of these operators are

$$\langle \alpha; na|\hat{r}_c|\alpha; na\rangle = na,$$

$$\langle s; na|\hat{r}_{\rm inter}|p; na\rangle = \rho, \tag{13}$$

where ρ is real. In the Bloch basis, $\hat{r}_c$ has no matrix representation because it includes intraband effects (its matrix thus diverges); its commutator with the Hamiltonian is, however, well-defined,

$$\hat{p}_k = \frac{m_0}{i\hbar}[\hat{r}_c, \hat{H}], \tag{14}$$

so that the matrix for this commutator is just $\overleftrightarrow{\mathbf{p}}_k = (m_0/\hbar)d\overleftrightarrow{\mathbf{H}}/dk$. On the other hand, $\hat{r}_{\rm inter}$ is a purely interband operator and hence has a well-defined Bloch basis matrix, and corresponding additional momentum matrix,

$$\overleftrightarrow{\mathbf{r}}_{\rm inter} = \begin{bmatrix} 0 & \rho \\ \rho & 0 \end{bmatrix}, \tag{15}$$

so that

$$\overleftrightarrow{\mathbf{p}}_{\rm inter} = \frac{m_0}{i\hbar}[\overleftrightarrow{\mathbf{r}}_{\rm inter}, \overleftrightarrow{\mathbf{H}}]. \tag{16}$$

We see immediately that because this matrix is well defined the added momentum does not affect expectation values. For example,

$$\frac{m_0}{i\hbar}\mathbf{v}_-^\dagger[\overleftrightarrow{\mathbf{r}}_{\rm inter}, \overleftrightarrow{\mathbf{H}}]\mathbf{v}_- = \frac{m_0}{i\hbar}[E_-(k) - E_-(k)]\mathbf{v}_-^\dagger \overleftrightarrow{\mathbf{r}}_{\rm inter}\mathbf{v}_- = 0, \tag{17}$$

since the expectation value of $\overleftrightarrow{\mathbf{r}}_{\rm inter}$ is finite. Thus it would seem that this prescription could be employed to adjust the interband momentum matrix element to the desired value via the real parameter ρ. Unfortunately, this prescription together with incompleteness leads to conclusions sharply at variance with atomic physics. This problem is especially serious in three dimensions so we shall also examine the elemental semiconductor sp^3 nearest-neighbor model having an extra same-atom *s*-*p* parameter satisfying relations analogous to

$$\langle s; \mathbf{R}_j|\hat{r}^{(x)}_{\rm inter}|x; \mathbf{R}_j\rangle = \langle s; \mathbf{R}_j|\hat{r}^{(y)}_{\rm inter}|y; \mathbf{R}_j\rangle = \langle s; \mathbf{R}_j|\hat{r}^{(z)}_{\rm inter}|z; \mathbf{R}_j\rangle = \rho, \tag{18}$$

where we label the three *p* orbitals x, y, z.

As mentioned above, the errors are associated with products of position operators so we first consider matrix elements of the operator $\hat{r}^2_{\rm inter}$, which cannot be treated as separate fitting parameters if we are to have a useful formalism. That is, if the matrices $\overleftrightarrow{\mathbf{r}}^2_{\rm inter}$ and $\overleftrightarrow{\mathbf{r}}_{\rm inter}\cdot\overleftrightarrow{\mathbf{r}}_{\rm inter}$ are not identical then in the formalism we can never be certain how to interpret higher powers of position. In Appendix A we show, for example, that the relation used in deriving the Baker-Hausdorff identity,

$$[\hat{r},[\hat{r},\hat{H}]] = \hat{r}^2\hat{H} - 2\hat{r}\hat{H}\hat{r} + \hat{H}\hat{r}^2 \tag{19}$$

(where $\hat{r} = \hat{r}_c + \hat{r}_{\rm inter}$ and for simplicity the model is the linear chain above), must hold if the model is to give the correct band curvatures. Calculating matrix elements of $\hat{r}^2_{\rm inter}$ with the enlarged tight-binding model Eq. (13) then leads to some rather startling conclusions, for both the linear chain,

$$\begin{aligned}\langle s;n'a|\hat{r}^2_{\mathrm{inter}}|s;na\rangle &= \sum_{\alpha,l}\,\langle s;n'a|\hat{r}_{\mathrm{inter}}|\alpha;la\rangle\\ &\quad\times\langle\alpha;la|\hat{r}_{\mathrm{inter}}|s;na\rangle\\ &= \rho^2\delta_{n',n}\,,\end{aligned}\tag{20}$$

$$\begin{aligned}\langle p;n'a|\hat{r}^2_{\mathrm{inter}}|p;na\rangle &= \sum_{\alpha,l}\,\langle p;n'a|\hat{r}_{\mathrm{inter}}|\alpha;la\rangle\\ &\quad\times\langle\alpha;la|\hat{r}_{\mathrm{inter}}|p;na\rangle\\ &= \rho^2\delta_{n',n}\,,\end{aligned}\tag{21}$$

and the sp^3 nearest-neighbor models,

$$\langle s;\mathbf{R}_j|\hat{r}^{(z)2}_{\mathrm{inter}}|s;\mathbf{R}_j\rangle=\langle z;\mathbf{R}_j|\hat{r}^{(z)2}_{\mathrm{inter}}|z;\mathbf{R}_j\rangle=\rho^2,\tag{22}$$

$$\langle x;\mathbf{R}_j|\hat{r}^{(z)2}_{\mathrm{inter}}|x;\mathbf{R}_j\rangle=0.\tag{23}$$

Equations (20)–(23) are, from an atomic physics perspective, unphysical, and are purely a consequence of the incomplete basis. Note the uneven treatment of the p orbitals: Equation (23) vanishes whereas properties of the spherical harmonics require $\langle x;\mathbf{R}_j|\hat{r}^{(z)2}_{\mathrm{inter}}|x;\mathbf{R}_j\rangle=(1/3)\langle z;\mathbf{R}_j|\hat{r}^{(z)2}_{\mathrm{inter}}|z;\mathbf{R}_j\rangle$ for true atomic orbitals. These sorts of problems appear to persist even if d orbitals are added: Although the inaccuracy in the s- and p-matrix elements is partially repaired, false-zero matrix elements like Eq. (23) now occur between d orbitals.

In addition, the enlarged tight-binding method in three dimensions leads to unphysical matrices for higher powers of position. In the localized-orbital basis the position operators for such a model are block diagonal in the atom location. Denoting by the subscript j,j the (s,x,y,z) block for the jth atom, the elemental semiconductor sp^3 nearest-neighbor model with a same-atom s-p parameter, Eq. (18), has matrix products

$$[\overleftrightarrow{\mathbf{r}}^{(x)}\overleftrightarrow{\mathbf{r}}^{(y)}]_{j,j}=\begin{bmatrix} R_j^{(x)}R_j^{(y)} & \rho R_j^{(y)} & \rho R_j^{(x)} & 0\\ \rho R_j^{(y)} & R_j^{(x)}R_j^{(y)} & \rho^2 & 0\\ \rho R_j^{(x)} & 0 & R_j^{(x)}R_j^{(y)} & 0\\ 0 & 0 & 0 & R_j^{(x)}R_j^{(y)}\end{bmatrix},\tag{24}$$

$$[\overleftrightarrow{\mathbf{r}}^{(y)}\overleftrightarrow{\mathbf{r}}^{(x)}]_{j,j}=\begin{bmatrix} R_j^{(x)}R_j^{(y)} & \rho R_j^{(y)} & \rho R_j^{(x)} & 0\\ \rho R_j^{(y)} & R_j^{(x)}R_j^{(y)} & 0 & 0\\ \rho R_j^{(x)} & \rho^2 & R_j^{(x)}R_j^{(y)} & 0\\ 0 & 0 & 0 & R_j^{(x)}R_j^{(y)}\end{bmatrix}.\tag{25}$$

Immediately we see that $\overleftrightarrow{\mathbf{r}}^{(x)}$ and $\overleftrightarrow{\mathbf{r}}^{(y)}$ no longer commute, which affects even the linear response (see Sec. III below) since as a result

$$[\hat{r}^{(x)},[\hat{r}^{(y)},\hat{H}^0]]\neq[\hat{r}^{(y)},[\hat{r}^{(x)},\hat{H}^0]].\tag{26}$$

This noncommutativity (i) implies a loss of gauge invariance for this formulation since now

$$\begin{aligned}&\exp\left\{\left(\frac{ie}{\hbar}\right)[A^{(x)}(t)\hat{r}^{(x)}+A^{(y)}(t)\hat{r}^{(y)}]\right\}\\ &\quad\neq\exp\left\{\left(\frac{ie}{\hbar}\right)A^{(x)}(t)\hat{r}^{(x)}\right\}\exp\left\{\left(\frac{ie}{\hbar}\right)A^{(y)}(t)\hat{r}^{(y)}\right\},\end{aligned}\tag{27}$$

and (ii) renders the matrices $\overleftrightarrow{\mathbf{r}}^{(y)}\overleftrightarrow{\mathbf{r}}^{(x)}$ and $\overleftrightarrow{\mathbf{r}}^{(x)}\overleftrightarrow{\mathbf{r}}^{(y)}$ non-Hermitian. Finally, as seen above for intra-atomic matrix elements, the noncommutativity appears to remain even if d orbitals are added.

Enforcing the isolated atom limit for any finite tight-binding model is thus quite costly. By enlarging the momentum matrix with extra parameters, an inconsistent momentum matrix results. When extra position parameters are added intra-atomic matrix elements of higher powers of position become increasingly incorrect, and the position matrices no longer commute. As a corollary, gauge invariance is lost, errors occur in the linear response, and most of the commonly employed expressions must be rederived to eliminate all hidden assumptions of commutativity and hermiticity. The Peierls-coupling tight-binding method avoids all of these problems and inconsistencies and can be applied to a wide variety of molecules and solids so long as there is an actual spatial separation between the atoms. In the next section we show that this formulation can reproduce bona fide intramolecular transitions.

III. DIELECTRIC SUSCEPTIBILITY OF POLY(PARA-PHENYLENE)

As an illustrative example of the Peierls-coupling tight-binding method, we calculate the optical dielectric response for crystalline poly(para-phenylene) (PPP). By varying a single structural parameter, this system allows one to study optical absorption both in the limit of isolated molecules (phenyl rings, that is) as well as in the case of periodic states. To keep things as simple as possible, we neglect the weak interaction between chains and use the structural parameters for single PPP chains as obtained by *ab initio* calculations[24] and employ only a single π state per carbon site. In addition, only interactions $V_{i,j}=g_{i,j}(\theta)\hbar\eta/(m_0 l^2_{i,j})$ between nearest neighbors (distance $l_{i,j}$) and with[24] $\eta=-0.81$ are included in the calculation. The angular function $g_{i,j}(\theta)$ reflects the nonplanar configuration of PPP where two adjacent rings are tilted with respect to each other by a torsion angle θ. Thus we take $g_{i,j}(\theta)=1$ and $g_{i,j}(\theta)=\cos(\theta)$ for atoms on the same and adjacent phenyl rings, respectively. The structure of a PPP chain that is embedded in a crystal is shown schematically in Fig. 1 and is drawn with the correct setting angle of $\phi=62.1°$ with respect to the crystal axes $\hat{a},\hat{b},\hat{c}$.[24] The chain axis is taken along z and the length of a two-ring primitive cell is c. The carbon atoms are numbered $j=0,\ldots,11$ with displacements from the cell origin denoted by $\mathbf{d}_j$. Atom 0 lies at the cell origin $(\mathbf{d}_0=0)$ and atom 11 at

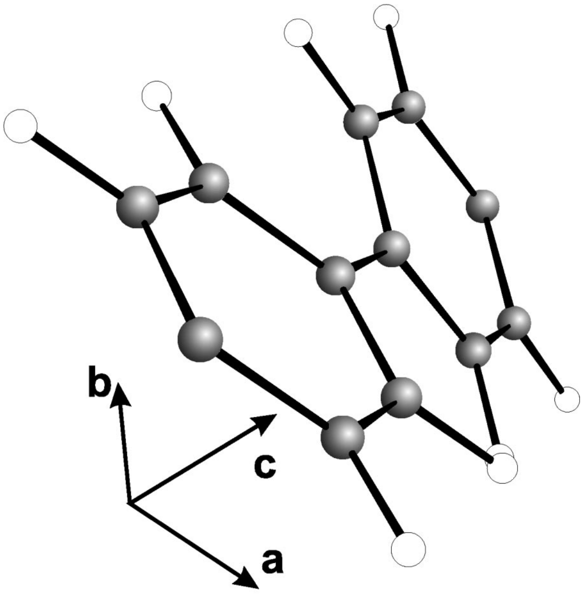

FIG. 1. Unit cell of one-dimensional PPP oriented in its crystalline setting relative to the directions a, b, c of the three-dimensional crystal. The two phenyl rings per unit cell are tilted with respect to each other. Gray (white) spheres represent C atoms (H atoms).

the opposite end of the cell so that atom 0 of cell L couples to atom 11 of cell $(L-1)$. The torsion angle θ between adjacent benzene rings determines the spatial localization of the eigenstates in the infinitely extended chain: for $\theta=0°$, the highest occupied (HOMO) and lowest occupied (LUMO) molecular orbital states are extended Bloch states along the chain axis, whereas for $\theta=90°$, the orthogonal orientation between π states on adjacent rings causes the eigenstates to be strictly intramolecular.

Since periodicity exists only in the z direction, we drop the index on the wave vector, denoting it simply as k, writing the Bloch basis for the PPP chain as

$$|\alpha;k\rangle=\frac{1}{\sqrt{N}}\sum_{L} e^{ikLc}|\alpha;L\rangle, \tag{28}$$

where $|\alpha;L\rangle$ is a π orbital located on atom $\alpha=0,\ldots,11$ in the Lth cell. In the Bloch basis, the matrix elements of the zero-field Hamiltonian are

$$\langle\alpha';k|\hat{H}^0|\alpha;k\rangle=V_{\alpha',\alpha}\exp(-ik\Lambda_{\alpha',\alpha}),$$

$$\Lambda_{\alpha',\alpha}=c[\delta_{\alpha',0}\delta_{\alpha,11}-\delta_{\alpha',11}\delta_{\alpha,0}]. \tag{29}$$

Diagonalizing $\hat{H}^0$ yields the eigenenergies and eigenstates (the band basis)

$$\hat{H}^0|n;k\rangle=E_n(k)|n;k\rangle,$$

$$|n;k\rangle=\sum_{\alpha} C_{n,\alpha}(k)|\alpha;k\rangle. \tag{30}$$

In the presence of the vector potential $\mathbf{A}(t)$ the matrix elements of the Hamiltonian in the localized-orbital basis are given by Eq. (2). Transforming to the Bloch basis yields, after some algebra,

$$\langle\alpha';k|\hat{H}|\alpha;k\rangle=\exp\left\{-\frac{ie}{\hbar}\mathbf{A}(t)\cdot(\mathbf{d}_{\alpha'}-\mathbf{d}_{\alpha}+\Lambda_{\alpha',\alpha}\mathbf{e}^{(z)})\right\}\times\langle\alpha';k|\hat{H}^0|\alpha;k\rangle, \tag{31}$$

where $\mathbf{e}^{(z)}$ denotes the unit vector along the chain axis. We note that the Bloch-basis matrix elements of $\hat{H}$ do not generally take such a simple form; this is especially the case if the system is periodic in more than one dimension. The Cartesian components of the current operator $\hat{j}^{(\mu)}(t)$ may now be found in one of two entirely equivalent ways. In the first we apply the defining relation $\hat{j}^{(\mu)}(t)=-\delta\hat{H}/\delta A^{(\mu)}(t)$ directly to the matrix elements Eq. (31), finding to first order in $\mathbf{A}$,

$$\langle\alpha';k|\hat{j}^{(\mu)}(t)|\alpha;k\rangle=-\frac{e}{m_0}\langle\alpha';k|\hat{p}^{(\mu)}|\alpha;k\rangle-\frac{e^2}{m_0}\sum_{\nu}\langle\alpha';k|\hat{T}^{(\mu),(\nu)}|\alpha;k\rangle A^{(\nu)}(t), \tag{32}$$

where

$$\langle\alpha';k|\hat{p}^{(\mu)}|\alpha;k\rangle=\frac{m_0}{i\hbar}(d_{\alpha'}^{(\mu)}-d_{\alpha}^{(\mu)}+\Lambda_{\alpha',\alpha}\delta_{\mu,z})\langle\alpha';k|\hat{H}^0|\alpha;k\rangle, \tag{33}$$

$$\langle\alpha';k|\hat{T}^{(\mu),(\nu)}|\alpha;k\rangle=-\frac{m_0}{\hbar^2}(d_{\alpha'}^{(\mu)}-d_{\alpha}^{(\mu)}+\Lambda_{\alpha',\alpha}\delta_{\mu,z})\times(d_{\alpha'}^{(\nu)}-d_{\alpha}^{(\nu)}+\Lambda_{\alpha',\alpha}\delta_{\nu,z})\langle\alpha';k|\hat{H}^0|\alpha;k\rangle. \tag{34}$$

Before continuing, we emphasize that the $d_{\alpha}^{(\mu)}$ appearing in Eqs. (31)–(34) are not additional fitting parameters: They are displacements, fixed by the molecular structure. We reiterate that we encounter none of the problems found in Sec. II C above because the position operator is diagonal in the localized-orbital basis.

The second method computes $\hat{j}^{(\mu)}(t)=(-e/i\hbar)[\hat{r}^{(\mu)},\hat{H}]$ using the explicit operator expression for $\hat{H}$, expanded to first order in $\mathbf{A}$ in the electric dipole approximation:[6]

$$\hat{H}\approx\hat{H}^0+\frac{e}{m_0}\sum_{\nu} A^{(\nu)}(t)\hat{p}^{(\nu)}, \tag{35}$$

so that the current is

$$\hat{j}^{(\mu)}(t) = -\frac{e}{m_0}\hat{p}^{(\mu)} - \frac{e^2}{m_0}\sum_{\nu}\hat{T}^{(\mu),(\nu)}A^{(\nu)}(t), \tag{36}$$

where

$$\hat{p}^{(\mu)} = \frac{m_0}{i\hbar}[\hat{r}^{(\mu)}\hat{H}^0], \tag{37}$$

$$\hat{T}^{(\mu),(\nu)} = -\frac{m_0}{\hbar^2}[\hat{r}^{(\mu)},[\hat{r}^{(\nu)},\hat{H}^0]], \tag{38}$$

are the operators whose matrix elements are given in Eqs. (33) and (34). We emphasize that these two methods are entirely equivalent. In fact, the Bloch-basis matrix elements of $\hat{H}$ (which has terms to all orders in **A**) are identical to Eq. (31), whereby the position operator is diagonal in the localized-orbital basis,[6]

$$\langle\alpha';L'|\hat{r}^{(\mu)}|\alpha;L\rangle = (d_{\alpha}^{(\mu)} + cL\,\delta_{\mu,z})\,\delta_{\alpha',\alpha}\delta_{L',L}. \tag{39}$$

The dielectric susceptibility tensor follows from standard linear-response theory using the current operator Eq. (32) or Eq. (36). The diagonal components of the imaginary part are

$$\mathrm{Im}[\chi^{(\nu),(\nu)}] = \frac{e^2\pi}{\varepsilon_0 m_0^2\omega^2 abL_c} \times \sum_{n,n',k}[f_n(k) - f_{n'}(k)]|\langle n';k|\hat{p}^{(\nu)}|n;k\rangle|^2 \times \delta[\hbar\omega - E_{n'}(k) + E_n(k)], \tag{40}$$

where $f_n(k)$ is the Fermi-Dirac function for the nth band at wave vector k, a and b are the primitive PPP cell dimensions in the x-y plane, and $L_c = cN_z$ is the length of a chain containing N_z primitive cells. In Appendix B, we show that the following f-sum rule, similar to that for solids with three-dimensional periodicity,[4] may be derived for Eq. (40). For all directions ν, we find

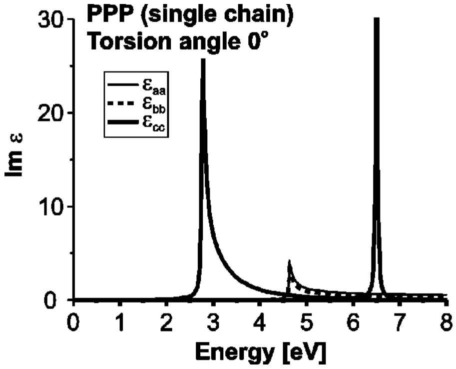

FIG. 2. Calculated components of the imaginary part of the dielectric function of one-dimensional PPP parallel to and perpendicular to the chain axis as a function of photon energy (in eV), for an artificial torsion angle of 0° between the two phenyl rings.

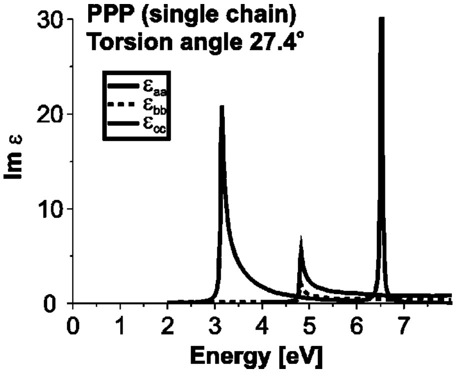

FIG. 3. Calculated components of the imaginary part of the dielectric function of one-dimensional PPP parallel to and perpendicular to the chain axis as a function of energy (in eV), for the realistic torsion angle of 27.4° between the two phenyl rings.

$$\int_0^{\infty}\omega\,\mathrm{Im}[\chi^{(\nu),(\nu)}]d\omega = \frac{e^2\pi}{2\varepsilon_0 m_0 abL_c}\sum_{n=1}^{N_v}\sum_{k}\langle n;k|\hat{T}^{(\nu),(\nu)}|n;k\rangle, \tag{41}$$

where the valence bands are numbered $1,\ldots,N_v$ and the sum over k runs covers the one-dimensional Brillouin zone. This relation provides an important consistency check in any numerical implementation.

In Figs. 2–4 we plot, as a function of photon energy, the imaginary part of the dielectric function for three different torsion angles $\theta = 0$, 27.4, and 90°; we have introduced a small Landau damping of 0.02 eV in the dielectric tensor to better show the relative strength of the absorption peaks. The calculations for the experimental torsion angle of 27.4° agree fairly well with electron-energy-loss spectroscopy (EELS) (Ref. 25) and optical absorption experiments[26] for the dielectric function component ε_{cc} with polarization along the chain as can be deduced from Fig. 5, given the extreme simplicity of the model. In particular, the position of both the main

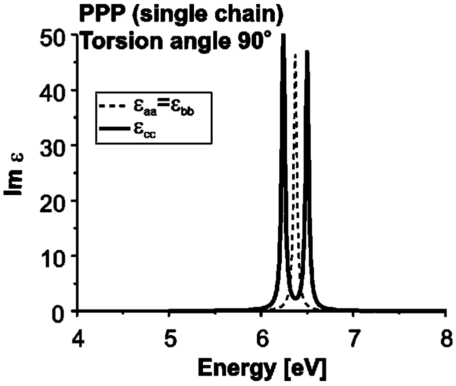

FIG. 4. Calculated components of the imaginary part of the dielectric function of one-dimensional PPP parallel to and perpendicular to the chain axis as a function of energy (in eV), for an artificial torsion angle of 90° which leads to effectively decoupled benzene molecules. Note the change in scale compared to the previous figures.

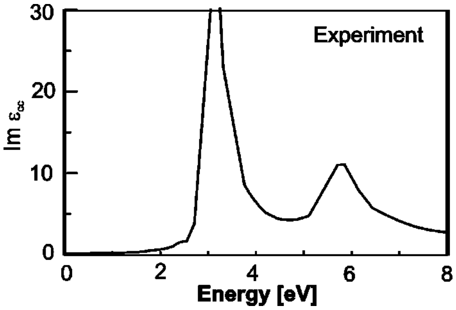

FIG. 5. Experimental imaginary part of the dielectric function of crystalline PPP parallel to the chain axis as a function of energy (in eV) (Ref. 25).

absorption peak at 3 eV and the secondary maximum at 6 eV agree well with experiment, the latter peak being much too narrow since it is strictly intramolecular in the present model. Adsorbance data on oriented PPP suggest a ratio of $\varepsilon_{cc}/\varepsilon_{aa}\sim 5$ near the absorption edge[26] which also agrees qualitatively with the present model. Figure 4 (torsion angle 90°) represents the limit of isolated benzene molecules. All lines represent intraphenyl $\pi-\pi^*$ transitions. The eigenstates within a phenyl ring can be classified as on-axis states, i.e., states that are localized mainly on the two chain-axis atoms, and off-axis states that are localized on the remaining four off-axis atoms. For ε_{cc}, one gets two dipole allowed transitions, one on-axis $\pi(\mathrm{on})\rightarrow\pi^*(\mathrm{on})$ and one off-axis $\pi(\mathrm{off})\rightarrow\pi^*(\mathrm{off})$ which have slightly different energies. For $\varepsilon_{aa}=\varepsilon_{bb}$, on the other hand, only the transition $\pi(\mathrm{on})\rightarrow\pi^*(\mathrm{off})$ and its degenerate counterpart $\pi(\mathrm{off})\rightarrow\pi^*(\mathrm{on})$ is dipole allowed as one can easily deduce from the geometry of the phenyl rings. This explains the results shown in Fig. 4. The present simple model neglects excitons which are known to modify the absorption significantly close to the band gap[27] but their effect is probably small on the energy scale shown in the figures.

We emphasize that the limiting case of isolated molecules (Fig. 4) shows that the Peierls-coupling tight-binding easily models true, intramolecular transitions, since there are no extended states in this case. So long as there is a true separation between the atoms and it is treated as in Eq. (39) above we recover the isolated molecule case without any of the inconsistencies associated with enlarging the model with extra, off-diagonal position parameters.

IV. CONCLUSIONS

We have generalized our previous Peierls-coupling tight-binding approach to electromagnetic interactions to encompass molecular solids and isolated molecules. In doing so we have examined in detail consequences of various prescriptions for the position and momentum operators in tight binding. We have shown that the only specification of the position operator which does not suffer from incompleteness-related problems is as a same-atom, same-orbital only interaction giving the atom location. We have also shown that attempting to fit parameters of the momentum matrix directly generally results in a momentum operator which is incompatible with the underlying tight-binding model, while adding extra position parameters results in numerous difficulties, including the loss of gauge invariance. We have applied our generalized results to the molecular solid PPP, showing that even in the limit of isolated molecules, the Peierls approach to tight-binding still reproduces intramolecular transitions.

ACKNOWLEDGMENTS

We thank Professor Brad Foreman for his comments on an earlier version of the manuscript. P.V. acknowledges support from the Office of Naval Research under Contract No. N00014-01-1-0242, and the Deutsche Forschungs-Gemeinschaft under SFB 348.

APPENDIX A: EFFECTIVE MASS FOR THE LINEAR CHAIN MODEL

Here we calculate the band curvature (inverse effective mass) at $k=0$ in the linear chain model of Secs. II B and II C including a same-atom s-p parameter in order to show that the matrix elements of $\overleftrightarrow{\mathbf{r}}^2_{\mathrm{inter}}$ and $\overleftrightarrow{\mathbf{r}}_{\mathrm{inter}}\cdot\overleftrightarrow{\mathbf{r}}_{\mathrm{inter}}$ must be identical for the model to give the correct curvature. First, we calculate the curvature directly from the eigenvalue, Eq. (8):

$$\left.\frac{d^2E_+(k)}{dk^2}\right|_{k=0}=-2a^2U_{ss}+\frac{8a^2U_{sp}^2}{(E_s-E_p)+2(U_{ss}-U_{pp})}. \tag{A1}$$

The curvature may also be calculated directly from the eigenvectors of the Hamiltonian Eq. (6),

$$\left.\frac{d^2E_+(k)}{dk^2}\right|_{k=0}=-\mathbf{v}_{0,+}^{\dagger}[\overleftrightarrow{\mathbf{r}},[\overleftrightarrow{\mathbf{r}},\overleftrightarrow{\mathbf{H}}]]\mathbf{v}_{0,+}+2\frac{|\mathbf{v}_{0,+}^{\dagger}[\overleftrightarrow{\mathbf{r}},\overleftrightarrow{\mathbf{H}}]\mathbf{v}_{0,-}|^2}{E_+(0)-E_-(0)}, \tag{A2}$$

where the eigenvalues and eigenvectors at $k=0$ are given by

$$E_+(0)=E_s+2U_{ss},\quad \mathbf{v}_{0,+}=\begin{bmatrix}1\\0\end{bmatrix},$$

$$E_-(0)=E_p+2U_{pp},\quad \mathbf{v}_{0,-}=\begin{bmatrix}0\\1\end{bmatrix}, \tag{A3}$$

and the matrix representations of the commutators are likewise evaluated at $k=0$. In this model the total position operator is a sum of two parts, $\hat{r}=\hat{r}_c+\hat{r}_{\mathrm{inter}}$, where $\hat{r}_c$ gives the atom location and thus diverges in the Bloch basis and $\hat{r}_{\mathrm{inter}}$ is the well behaved same-atom s-p interaction whose matrix is given in Eq. (15). Recall that although $\hat{r}_c$ diverges its commutator with the Hamiltonian is well-defined so that we get

$$[\overleftrightarrow{\mathbf{r}}_c,\overleftrightarrow{\mathbf{H}}]=i\frac{d\overleftrightarrow{\mathbf{H}}}{dk},$$

$$[\overleftrightarrow{\mathbf{r}}_c,[\overleftrightarrow{\mathbf{r}}_c,\overleftrightarrow{\mathbf{H}}]]=-\frac{d^2\overleftrightarrow{\mathbf{H}}}{dk^2}. \tag{A4}$$

Thus, at $k=0$,

$$\left.\frac{d\overleftrightarrow{\mathbf{H}}}{dk}\right|_{k=0}=\begin{bmatrix}0 & i2aU_{sp}\\ -i2aU_{sp} & 0\end{bmatrix},$$

$$\left.\frac{d^2\overleftrightarrow{\mathbf{H}}}{dk^2}\right|_{k=0}=\begin{bmatrix}-2a^2U_{ss} & 0\\ 0 & -2a^2U_{pp}\end{bmatrix}. \tag{A5}$$

Using Eqs. (6) and (15) it is easy to calculate

$$[\overleftrightarrow{\mathbf{r}}_{\text{inter}},\overleftrightarrow{\mathbf{H}}]_{k=0}=\begin{bmatrix}0 & -\rho[E_s-E_p+2(U_{ss}-U_{pp})]\\ \rho[E_s-E_p+2(U_{ss}-U_{pp})] & 0\end{bmatrix}, \tag{A6}$$

so that we have for the squared interband matrix element in Eq. (A2),

$$|\mathbf{v}_{0,+}^{\dagger}[\overleftrightarrow{\mathbf{r}},\overleftrightarrow{\mathbf{H}}]\mathbf{v}_{0,-}|^2=\{2aU_{sp}+\rho[E_s-E_p+2(U_{ss}-U_{pp})]\}^2. \tag{A7}$$

The first step in evaluating the double commutator in Eqs. (A1) and (A2) is expanding it:

$$\begin{aligned}[\overleftrightarrow{\mathbf{r}},[\overleftrightarrow{\mathbf{r}},\overleftrightarrow{\mathbf{H}}]]&=[\overleftrightarrow{\mathbf{r}}_c,[\overleftrightarrow{\mathbf{r}}_c,\overleftrightarrow{\mathbf{H}}]]+[\overleftrightarrow{\mathbf{r}}_c,[\overleftrightarrow{\mathbf{r}}_{\text{inter}},\overleftrightarrow{\mathbf{H}}]]+[\overleftrightarrow{\mathbf{r}}_{\text{inter}},[\overleftrightarrow{\mathbf{r}}_c,\overleftrightarrow{\mathbf{H}}]]\\&\quad+[\overleftrightarrow{\mathbf{r}}_{\text{inter}},[\overleftrightarrow{\mathbf{r}}_{\text{inter}},\overleftrightarrow{\mathbf{H}}]].\end{aligned} \tag{A8}$$

The first term in Eq. (A8) is given in Eq. (A4). For the second and third, we observe that commutators of $\hat{r}_c$ with cell-periodic operators corresponding to k-space differentiation as in Eq. (A4), and that the matrix $\overleftrightarrow{\mathbf{r}}_{\text{inter}}$ in Eq. (15) is k independent. The sum then simplifies to

$$\begin{aligned}&[\overleftrightarrow{\mathbf{r}}_c,[\overleftrightarrow{\mathbf{r}}_{\text{inter}},\overleftrightarrow{\mathbf{H}}]]|_{k=0}+[\overleftrightarrow{\mathbf{r}}_{\text{inter}},[\overleftrightarrow{\mathbf{r}}_c,\overleftrightarrow{\mathbf{H}}]]|_{k=0}\\&\quad=2i\left.\left[\overleftrightarrow{\mathbf{r}}_{\text{inter}},\frac{d\overleftrightarrow{\mathbf{H}}}{dk}\right]\right|_{k=0}=\begin{bmatrix}8a\rho U_{sp} & 0\\ 0 & -8a\rho U_{sp}\end{bmatrix}.\end{aligned} \tag{A9}$$

All that remains is the final double commutator, involving only the same-atom, s-p interaction. Evaluating this double commutator shows that the matrix elements of $\overleftrightarrow{\mathbf{r}}_{\text{inter}}^2$ cannot be chosen independently. This is established by observing that in atomic physics the expectation values of $\overleftrightarrow{\mathbf{r}}_{\text{inter}}^2$ for s and p orbitals need not be the same. Hence it ought to be the case that

$$\langle s;n'a|\hat{r}_{\text{inter}}^2|s;na\rangle=\eta_s^2\delta_{n',n},$$

$$\langle p;n'a|\hat{r}_{\text{inter}}^2|p;na\rangle=\eta_p^2\delta_{n',n}, \tag{A10}$$

with $\eta_s^2\neq\eta_p^2$. Expanding the double commutator

$$[\overleftrightarrow{\mathbf{r}}_{\text{inter}},[\overleftrightarrow{\mathbf{r}}_{\text{inter}},\overleftrightarrow{\mathbf{H}}]]=\overleftrightarrow{\mathbf{r}}_{\text{inter}}^2\overleftrightarrow{\mathbf{H}}-2\overleftrightarrow{\mathbf{r}}_{\text{inter}}\overleftrightarrow{\mathbf{H}}\overleftrightarrow{\mathbf{r}}_{\text{inter}}+\overleftrightarrow{\mathbf{H}}\overleftrightarrow{\mathbf{r}}_{\text{inter}}^2, \tag{A11}$$

and employing the prescriptions Eqs. (A10), (15), (16) then leads to

$$[\overleftrightarrow{\mathbf{r}}_{\text{inter}},[\overleftrightarrow{\mathbf{r}}_{\text{inter}},\overleftrightarrow{\mathbf{H}}]]_{k=0}=\begin{bmatrix}D_{sp} & 0\\ 0 & D_{ps}\end{bmatrix},$$

$$D_{sp}=2\eta_s^2(E_s+2U_{ss})-2\rho^2(E_p+2U_{pp}), \tag{A12}$$

$$D_{ps}=2\eta_p^2(E_p+2U_{pp})-2\rho^2(E_s+2U_{ss}),$$

where ρ is the same-orbital s-p parameter in Eq. (13). Combining Eqs. (A5), (A9), and (A12) gives

$$\begin{aligned}-\mathbf{v}_{0,+}^{\dagger}[\overleftrightarrow{\mathbf{r}},[\overleftrightarrow{\mathbf{r}},\overleftrightarrow{\mathbf{H}}]]\mathbf{v}_{0,+}&=-2a^2U_{ss}-8a\rho U_{sp}-2\eta_s^2\\&\quad\times(E_s+2U_{ss})+2\rho^2(E_p+2U_{pp}),\end{aligned} \tag{A13}$$

so that

$$\begin{aligned}&-\mathbf{v}_{0,+}^{\dagger}[\overleftrightarrow{\mathbf{r}},[\overleftrightarrow{\mathbf{r}},\overleftrightarrow{\mathbf{H}}]]\mathbf{v}_{0,+}+2\frac{|\mathbf{v}_{0,+}^{\dagger}[\overleftrightarrow{\mathbf{r}},\overleftrightarrow{\mathbf{H}}]\mathbf{v}_{0,-}|^2}{E_+(0)-E_-(0)}\\&\quad=-2a^2U_{ss}+\frac{8a^2U_{sp}^2}{(E_s-E_p)+2(U_{ss}-U_{pp})}+2(\rho^2-\eta_s^2)\\&\qquad\times(E_s+2U_{ss}).\end{aligned} \tag{A14}$$

It is obvious that Eq. (A14) can only give the correct curvature Eq. (A1) if $\eta_s^2=\rho^2$. Hence the matrix elements of $\overleftrightarrow{\mathbf{r}}_{\text{inter}}^2$ cannot be treated as independent fitting parameters, contrary to what is suggested by atomic physics.

APPENDIX B: *f*-SUM RULE FOR THE PPP CHAIN

We begin with the susceptibility for the PPP chain,

$$\mathrm{Im}[\chi^{(\beta),(\beta)}]=\frac{e^2\pi}{\varepsilon_0 m_0^2\omega^2 abL_c}\times\sum_{n,n',k}[f_n(k)-f_{n'}(k)]|\langle n';k|\hat{p}^{(\beta)}|n;k\rangle|^2\times\delta[\hbar\omega-E_{n'}(k)+E_n(k)]. \tag{B1}$$

At $T=0$ all of the Fermi factors become 0 or 1, and the double sums simplify since the difference of Fermi factors is zero for n and n' both valence or both conduction bands. Integrating $\omega\mathrm{Im}[\chi^{(\beta),(\beta)}(\omega)]$ over the interval $\omega\in[0,\infty)$ picks out positive frequencies, so that the only terms to survive are those for which the sum over n covers the valence bands and that over n' covers the conduction bands. Using

$$\langle n';k|\hat{p}^{(\mu)}|n;k\rangle=\frac{m_0}{i\hbar}\langle n';k|\hat{r}^{(\mu)}|n;k\rangle[E_n(k)-E_{n'}(k)], \tag{B2}$$

and symmetrizing the sum (hence the factor of 2 in the denominator) we have

$$\int_0^\infty\omega\mathrm{Im}[\chi^{(\beta),(\beta)}]d\omega=\frac{e^2\pi}{2\varepsilon_0 m_0^2 abL_c}\left(\frac{m_0}{i\hbar}\right)\times\sum_{n=1}^{N_v}\sum_{n'=N_v+1}^{N_b}\sum_k[\langle n;k|\hat{r}^{(\beta)}|n';k\rangle\langle n';k|\hat{p}^{(\beta)}|n;k\rangle-\langle n;k|\hat{p}^{(\beta)}|n';k\rangle\langle n';k|\hat{r}^{(\beta)}|n;k\rangle], \tag{B3}$$

where there are N_b bands in the model and the bands $1,\dots,N_v$ are valence bands. We next add and subtract a term that is obtained from Eq. (B3) by changing the summation index of the middle sum to $n'=1,\dots,N_v$. The added term is absorbed into Eq. (B3) so that the sum over n' now covers all the bands, $n'=1,\dots,N_b$. The sum over the states $|n';k\rangle$ is now nothing more than the finite-basis closure relation and may be removed, leaving a sum over the diagonal matrix elements $\langle n;k|\hat{T}^{(\beta),(\beta)}|n;k\rangle$. The term that we subtracted is readily simplified as well. Because both n and n' are summed over all valence bands, for each pair $(n,n')=(j,j')$ there is another $(n,n')=(j',j)$ which gives an equal but opposite contribution; hence no interband matrix elements survive. What remains is a sum over the matrix elements of operators which are purely intraband in the band basis,

$$\frac{e^2\pi}{2\varepsilon_0 m_0^2 abL_c}\left(\frac{m_0}{i\hbar}\right)\sum_{n=1}^{N_v}\sum_{n'=1}^{N_v}\sum_k\{\langle n;k|\hat{r}^{(\beta)}|n';k\rangle\times\langle n';k|\hat{p}^{(\beta)}|n;k\rangle-\langle n;k|\hat{p}^{(\beta)}|n';k\rangle\langle n';k|\hat{r}^{(\beta)}|n;k\rangle\}$$
$$=\frac{e^2\pi}{2\varepsilon_0 m_0^2 abL_c}\left(\frac{m_0}{i\hbar}\right)\sum_{n=1}^{N_v}\sum_k\{\langle n;k|\hat{r}^{(\beta)}_{\mathrm{intra}}|n;k\rangle\times\langle n;k|\hat{p}^{(\beta)}_{\mathrm{intra}}|n;k\rangle-\langle n;k|\hat{p}^{(\beta)}_{\mathrm{intra}}|n;k\rangle\langle n;k|\hat{r}^{(\beta)}_{\mathrm{intra}}|n;k\rangle\}, \tag{B4}$$

since $\langle n;k|\hat{r}^{(\beta)}|n;k\rangle=\langle n;k|\hat{r}^{(\beta)}_{\mathrm{intra}}|n;k\rangle$, etc. For the PPP chain we must distinguish two cases: $\beta=x,y$, for which there is no translational periodicity and $\beta=z$, for which there is translational periodicity: The only potential difficulty surrounds the matrix elements of position which are divergent for directions in which periodicity exists. For the case $\beta=x,y$, the band-basis matrix elements of position are bounded since using Eq. (39) gives bounded Bloch-basis matrix elements

$$\langle\alpha';k|\hat{r}^{(\beta)}|\alpha;k\rangle=\frac{1}{N_z}\sum_{L'}\sum_L e^{ikc(L-L')}\langle\alpha';L'|\hat{r}^{(\beta)}|\alpha;L\rangle=\delta_{\alpha',\alpha}d_\alpha^{(\beta)}, \tag{B5}$$

and the band-basis states are simply well-behaved linear combinations of the Bloch-basis states. Because the intraband momentum matrix elements are well behaved for both x and y, the term in curly braces on the right-hand side of Eq. (B4) vanishes for all n and Eq. (B4) gives zero.

For $\beta=z$, we must treat the matrix elements of position in Eq. (B4) as k-space operators:[28]

$$\langle n;k|\hat{r}^{(\beta)}_{\mathrm{intra}}|n;k\rangle=i\frac{\partial}{\partial k^{(\beta)}}+\Xi^{(\beta)}_{n,n}, \tag{B6}$$

where $\Xi^{(\beta)}_{n,n}$ is the expectation value of $i\partial/\partial k^{(\beta)}$ taken with respect to the periodic part of $|n;k\rangle$. Since

$$\langle n;k|\hat{p}^{(\beta)}_{\mathrm{intra}}|n;k\rangle=\frac{m_0}{\hbar}\frac{\partial E_n(k)}{\partial k^{(\beta)}}, \tag{B7}$$

we have

$$\langle n;k|\hat{r}^{(\beta)}_{\mathrm{intra}}|n;k\rangle\langle n;k|\hat{p}^{(\beta)}_{\mathrm{intra}}|n;k\rangle-\langle n;k|\hat{p}^{(\beta)}_{\mathrm{intra}}|n;k\rangle\langle n;k|\hat{r}^{(\beta)}_{\mathrm{intra}}|n;k\rangle=\left(i\frac{\partial}{\partial k^{(\beta)}}+\Xi^{(\beta)}_{n,n}\right)\frac{m_0}{\hbar}\frac{\partial E_n(k)}{\partial k^{(\beta)}}-\frac{m_0}{\hbar}\frac{\partial E_n(k)}{\partial k^{(\beta)}}\left(i\frac{\partial}{\partial k^{(\beta)}}+\Xi^{(\beta)}_{n,n}\right)=i\frac{m_0}{\hbar}\frac{\partial^2E_n(k)}{\partial k^{(\beta)}\partial k^{(\beta)}}, \tag{B8}$$

so that

$$\frac{e^2\pi}{2\varepsilon_0 m_0^2 abL_c}\left(\frac{m_0}{i\hbar}\right)\sum_{n=1}^{N_v}\sum_{n'=1}^{N_v}\sum_{k}\,[\langle n;k|\hat{r}^{(\beta)}|n';k\rangle \times\langle n';k|\hat{p}^{(\beta)}|n;k\rangle-\langle n;k|\hat{p}^{(\beta)}|n';k\rangle\langle n';k|\hat{r}^{(\beta)}|n;k\rangle] =\frac{e^2\pi}{2\varepsilon_0 m_0^2 abL_c}\left(\frac{m_0}{i\hbar}\right)\left(\frac{im_0}{\hbar}\right)\sum_{n=1}^{N_v}\sum_{k}\frac{\partial^2 E_n(k)}{\partial k^{(\beta)}\partial k^{(\beta)}}. \tag{B9}$$

For a large system we convert the sum over the (one-dimensional) Brillouin zone into an integral, and since $E_n(k)$ is periodic over the zone the integral of its second derivative vanishes.[29] In all three directions, then, the term added to Eq. (B3) with the sum over n' running from $n'=1,\ldots,N_v$ contributes nothing and we arrive at the *f*-sum rule for the PPP chain as

$$\int_0^\infty \omega \mathrm{Im}[\chi^{(\beta),(\beta)}]d\omega =\frac{e^2\pi}{2\varepsilon_0 m_0 abc}\frac{1}{N_z}\sum_{n=1}^{N_v}\sum_{k}\,\langle n;k|\hat{T}^{(\beta),(\beta)}|n;k\rangle, \tag{B10}$$

where c is the dimension along the z direction (not the speed of light).

---

[1] W. A. Harrison, *Elementary Electronic Structure* (World Scientific, Singapore, 1999).

[2] *Tight-Binding Approach to Computational Materials Science*, edited by P. E. A. Turchi, A. Gonis, and L. Colombo, Mater. Res. Soc. Symp. Proc. No. 491 (Materials Research Society, Warrendale, 1999).

[3] J. A. Majewski and P. Vogl, in *Quantum Theory of Structure: Tight-Binding Systems*, edited by F. R. de Boer and D. G. Pettifor (North-Holland, Amsterdam, 1989), p. 287.

[4] M. Graf and P. Vogl, Phys. Rev. B **51**, 4940 (1995); M. Graf, Ph.D. thesis, Technical University of Munich, 1996.

[5] Timothy B. Boykin, Phys. Rev. B **60**, 15 810 (1999).

[6] Timothy B. Boykin, R. C. Bowen, and Gerhard Klimeck, Phys. Rev. B **63**, 245314 (2001).

[7] Timothy B. Boykin, Phys. Rev. B **52**, 16 317 (1995).

[8] P. Vogl, M. Graf, and A. Görling, in *Tight-Binding Approach to Computational Materials Science* (Ref. 2), p. 241.

[9] A. Di Carlo, S. Pescetelli, M. Pacioti, and P. Lugli, Solid State Commun. **98**, 803 (1996).

[10] Thomas Garm Pedersen, Kjeld Pedersen, and Thomak Brun Kriestensen, Phys. Rev. B **63**, 201101 (2001).

[11] R. E. Allen, T. Dumitrica, and B. Torralva, in *Ultrafast Physical Processes in Semiconductors*, edited by K. T. Tsen (Academic, New York, 2001), Chap. 7.

[12] T. Dumitrica and R. E. Allen, Solid State Commun. **113**, 653 (2000).

[13] T. Dumitrica, J. S. Graves, and R. E. Allen, Phys. Rev. B **58**, 15 340 (1998).

[14] Gi-Yeong Oh, Phys. Rev. B **63**, 087301 (2001).

[15] H. N. Nazareno and P. E. de Brito, Phys. Rev. B **64**, 045112 (2001).

[16] T. Dröse, M. Batsch, Isa Kh. Zharekeshev, and B. Kramer, Phys. Rev. B **57**, 37 (1998).

[17] B. Lindquist and R. Riklund, Phys. Rev. B **60**, 10 054 (1999).

[18] A. P. Horsfield, Phys. Rev. B **56**, 6594 (1997).

[19] Yu. Kontsevoi, O. N. Mryasov, A. I. Likhtenshtein, and V. A. Gubanov, Fiz. Tverd. Tela **34**, 126 (1992) [Sov. Phys. Solid State **34**, 154 (1992)].

[20] O. K. Andersen, Z. Pawlowska, and O. Jepsen, Phys. Rev. B **34**, 5253 (1986).

[21] M. Elstner, D. Porezag, G. Jungnickel, J. Elsner, M. Haugk, T. Frauenheim, S. Suhai, and G. Seifert, Phys. Rev. B **58**, 7260 (1998).

[22] R. W. Nunes and D. Vanderbilt, Phys. Rev. Lett. **73**, 712 (1994).

[23] A. Selloni, P. Marsella, and R. Del Sole, Phys. Rev. B **33**, 8885 (1986).

[24] C. Ambrosch-Draxl, J. A. Majewski, P. Vogl, and G. Leising, Phys. Rev. B **51**, 9668 (1995).

[25] J. Fink, Adv. Electron. Electron Phys. **75**, 121 (1989).

[26] N. Tanigaki, H. Kyotani, M. Wada, A. Kaito, Y. Yoshida, E. Han, K. Abe, and K. Yase, Thin Solid Films **331**, 229 (1998).

[27] M. Knupfer, T. Pichler, M. S. Golden, J. Fink, M. Murgia, R. H. Michel, R. Zamboni, and C. Taliani, Phys. Rev. Lett. **83**, 1443 (1999).

[28] E. I. Blount, in *Solid State Physics*, edited by Frederick Seitz and David Turnbull (Academic, New York, 1962), Vol. 13, p. 305.

[29] J. E. Sipe and Ed Ghahramani, Phys. Rev. B **48**, 11 705 (1993).